Indian Journal of Chemistry
Vol. 58A, February 2019, pp. 271-280

Studies on palladium based bimetallic catalysts Pd-M/TiO_2 (M = Cu, Ag & Au): I-Selective hydrogenation of 1-heptyne

A Saranya[a,b], G Vivekanandan[b], K Thirunavukkarasu[a], K R Krishnamurthy[a] & B Viswanathan[a,*]

[a]National Centre for Catalysis Research, Indian Institute of Technology, Madras, Chennai 600 036, India
[b]Department of Chemistry, A.V.C. College, Mannampandal, Mayiladuthurai, 609 305, India

Email: bviswanathan@gmail.com

Received 10 September 2018; accepted 15 January 2019

Two series of palladium based bi-metallic catalysts, $Pd_{(1-x)}Au_x$ (x = 0.1, 0.12, 0.15 and 0.2) and Pd_mM_n (M = Cu/Ag/Au; m, n = 0.9, 0.1) supported on TiO_2-P-25, have been prepared and characterized by X-ray diffraction (XRD), Diffuse Reflectance Spectroscopy (DRS), Transmission Electron Microscopy (TEM), X-ray Photo-electron Spectroscopy (XPS) and Temperature Programmed Reduction (TPR). DRS and XPS studies indicate formation of nano scale alloys involving redistribution of charges within the metals. Selective hydrogenation of 1-heptyne in liquid phase has been studied on these catalysts at atmospheric pressure and in the temperature range 293–313 K. In the $Pd_{(1-x)}Au_x$ series, the catalyst composition $Pd_{0.9}Au_{0.1}$ displays maximum activity, expressed as TOF. Activity pattern in $Pd_{0.9}M_{0.1}$ series follows the trend, Pd-Au > Pd-Ag = Pd-Cu > Pd. Selectivity for heptene formation is maintained at > 95% on all catalysts up to 60 min reaction time. Interplay of ensemble as well as ligand effects, acting simultaneously, influences the adsorption and activation of 1-heptyne, leading to higher activity on Pd-Au bimetallic catalyst vis-à-vis other bimetallic and mono metallic catalysts.

Keywords: Hydrogenation, 1-Heptyne, Bimetallic palladium catalysts, Ensemble, Ligand effects, Adsorption, Activation of 1-heptyne

Selective hydrogenation of alkynes to the corresponding alkenes has been studied extensively in view of its industrial applications as well as the scientific and technological challenges therein, for designing efficient catalysts, understanding of the reaction pathways and associated process features[1,2]. While the selective hydrogenation of C_2 to C_4 alkynes, to yield the corresponding alkenes, constitute a series of crucial catalytic processes[3] for purification and improving yields of basic petrochemicals (ethylene, propylene and 1,3-butadiene), hydrogenation of long chain alkynes (> C_5)[4] and alkynols[5] finds applications in pharmaceutical and fine chemicals manufacture. In this context, selective hydrogenation of 1-heptyne to heptene as a model reaction is being pursued in great detail[6-16]. Palladium based mono and bimetallic catalysts, have been studied extensively, to unravel the mode of functioning of the catalysts, improve activity and selectivity and optimize the hydrogenation process conditions. Choice of promoter elements[6-8], nature of metal precursors[9], supports, support nano structure and crystallite size[10-13], type of catalyst micro structures (alloys, egg-shell configurations)[14,15] and methods for preparation of catalysts[16, 17] could influence the activity, selectivity and stability.

Cu, Ag and Au are the commonly used promoters/second elements along with Pd for the selective hydrogenation of acetylene in ethylene rich streams[1-3]. For the hydrogenation of 1-heptyne, majority of the studies pertain to Pd-Au bimetallic catalysts[15,17] with only few on Pd-Cu[6] and Pd-Ag[8]. The nature and the degree of interactions (geometric and electronic) between Pd and Au (or any second metal) depend on the composition/atomic ratio of the bimetallic catalysts. Most of the studies, however, are concerned with fixed composition of Pd & Au[13,15,17]. Though improvements in the performance of Pd catalysts with these promoters have been observed, a comparative study to elucidate the superior performance of Pd-Au bi-metallic catalysts for selective hydrogenation of 1-heptyne is lacking. We have, therefore, carried out a systematic study, involving the optimization of Pd-Au atomic ratio and understanding of the relative efficacy of group IB metals, Cu, Ag and Au, as promoters for Pd based bi-metallic catalysts, in order to gain a better insight into the functionalities for selective hydrogenation of 1-heptyne. In $Pd_{(1-x)}Au_x$ series of catalysts, variation in compositions up to x = 0.2 has been considered since dilution effects and consequent decrease in conversion is observed at higher values of x[18].

Materials and Methods

Palladium chloride, poly vinyl pyrrolidone (PVP), auric chloride and 1-heptyne were obtained from Sigma Aldrich. Ethylene glycol (EG), sodium hydroxide (NaOH), silver nitrate, copper nitrate and methanol obtained from Qualigens were used as such.

Preparation of catalysts

Mono metallic Pd (1% *w*/*w*) and bimetallic nano particles $Pd_{(1-x)}Au_x$ (with x = 0.10, 0.12, 0.15 and 0.2) and Pd_mM_n (M = Cu/Ag/Au, m = 0.9 and n = 0.1) supported on titania (P-25) were prepared by the reduction of H_2 $PdCl_4$ by ethylene glycol, in presence of NaOH and PVP as the stabilizer[19]. Typically, 16.5 mg of $PdCl_2$ (0.059 mmol Pd) and 25 µL of concentrated HCl were mixed well in a 100 mL glass beaker to get H_2PdCl_4. A solution containing 25 mg of PVP (0.625 µmol) and 6 mL of ethylene glycol was added, followed by the addition of 0.75 mL of 0.31 M NaOH to H_2PdCl_4 solution. The mixture was stirred for half an hour at 60 °C to obtain a black colloidal suspension of Pd. To the Pd colloidal solution, 0.99 g of TiO_2 (P-25) was added slowly and the temperature was increased to 110 °C using an oil bath. The mixture was stirred continuously, till ethylene glycol was expelled. The catalyst was then dried in hot air oven overnight at 100 °C to get mono metallic Pd/TiO_2.

Two sets of bimetallic catalysts, the first, $Pd_{(1-x)}Au_x$ with x = 0.1, 0.12, 0.15 and 0.2 and the second, Pd_mM_n with M = Cu/Ag/Au and m and n values of 0.9 and 0.1 were prepared. Bimetallic catalysts of $Pd_{(1-x)}$ Au_x series were prepared by taking appropriate quantities of $PdCl_2$ and $HAuCl_4$. For the preparation of Pd-M (M = Cu/Ag/Au) catalysts, appropriate quantities of $PdCl_2$ and second metal salt (s) ($Cu(NO_3)_2.5H_2O$/$AgNO_3$/$HAuCl_4$) were taken. In both cases Pd and the second metal salts were added to the impregnation solution prior to reduction by ethylene glycol. Reduction and further treatment carried out were similar to that adopted for monometallic Pd catalyst.

Characterization of catalysts

Powder XRD diffraction patterns for the catalysts were recorded by using Rigaku Miniflex II X-ray diffractometer with Cu-Kα (λ = 0.15418 nm) radiation in the 2θ range of 10º to 80º and at a scan rate of 3º/min.

Temperature Programmed Reduction (H_2-TPR) studies were carried out using Micromeritics Autochem II 2920 chemisorption analyser. For TPR, the catalysts were calcined in air at 300 °C, prior to TPR experiments. The calcined catalyst (50 mg) was pre-treated at 300 ºC in high purity Ar gas (25 cc/min) for 1 h and then cooled to room temperature in Ar flow. The gas was changed to 10% H_2 in Ar (25 cc/min) at room temperature. After the stabilization of the baseline, TPR was started from RT to 700 ºC with a heating rate 10 ºC/min.

Transmission electron micrographs were recorded using JEOL 3010 model microscope. Few milligrams of the reduced samples (1–2 mg) were dispersed in few mL (1–2 mL) of ethanol by ultra-sonication for 15 min and a drop of the dispersion was placed on a carbon coated copper grid and allowed to dry in air at room temperature. Based on the mean particle size measured from TEM data, Pd metal dispersion was calculated using the formula[20]

$$\text{Dispersion}(\%) = \frac{600 \times M_{Pd}}{\rho_{Pd} \times d_{nm} \times a_{Pd} \times N_a} \quad \ldots (1)$$

where, M_{Pd} is the molecular weight of Pd (106.4 g/mol), a_{Pd} is the atomic surface area of Pd (6.8×10^{-20} m^2/atom), ρ_{pd} is the density of Pd (12.02 g/cm^3), N_a is Avogadro's number, and d_{nm} is the average particle diameter (in nm) estimated from TEM data.

X-ray photoelectron spectra of the reduced catalysts were recorded using Omicron Nanotechnology instrument with Mg-Kα radiation. The base pressure of the analysis chamber during the scan was 2×10^{-10} millibar. The pass energies for individual scan and survey scan are 20 and 100 eV, respectively. The spectra were recorded with a step width of 0.05 eV. The data were processed with the Casa XPS.

DR spectra for the reduced catalysts in the UV-visible region were recorded using a Thermo Scientific Evolution 600 spectrophotometer equipped with a Praying Mantis DRS accessory.

Hydrogenation of 1-heptyne

Liquid phase hydrogenation of 1-heptyne was carried out in the temperature range 293–313K, at atmospheric pressure. Initially, 20 mg of catalyst was dispersed in 34.64 g (40 mL) of toluene in a three necked RB flask (Supplementary Data, Fig. S1). Hydrogen gas (20 mL/min) was bubbled continuously into toluene at 313 K for 2 h so as to maintain Pd in metallic state. Then, 0.6928 g of 1-heptyne (7.2 mmol or 1.96% *w*/*w* in toluene) was then added to initiate the reaction. Hydrogen flow was maintained throughout the reaction time (60 min). Stirring rate of

1000 rpm was maintained to eliminate mass transfer effects. Reactant and products were analyzed at regular time intervals by gas chromatography. Rates of hydrogenation (r) and Pd metal dispersion (calculated using eqn 1) values were utilized to compute turn over frequency (TOF) using eqn 2[19]

$$\mathrm{TOF}(s^{-1}) = \frac{r}{n_{tot} \times \mathrm{dispersion}(\%)} \quad \ldots (2)$$

where r is the rate of hydrogenation (moles converted per second), n_{tot} is the total number of Pd moles in the reactor.

Results and Discussion

$Pd_{(1-x)}Au_x/TiO_2$ series of bimetallic catalysts

No significant change in XRD patterns for $Pd_{(1-x)}Au_x/TiO_2$ series of catalysts (Fig. S2) is observed, due to low metal loading. All *d*-lines characteristic of TiO_2-P-25 phase were observed.

DRS profiles (Fig. 1) for the $Pd_{(1-x)}Au_x$ series of catalysts reveal the characteristic absorption band due to TiO_2-P-25 support at 395 nm. While the Surface Plasmon Resonance (SPR) band attributed to Au nano particles at 562 nm is observed in the spectrum for mono metallic Au/TiO_2, it is not observed in the spectra for bi-metallic $Pd_{(1-x)}Au_x$ series of catalysts. The absence of SPR band in bi-metallic catalysts could be attributed to the formation of Pd-Au nano scale alloys involving electronic interactions between Pd and Au[15,21,22].

Transmission electron micrographs for $Pd_{(1-x)}Au_x$ series of catalysts presented in Fig. 2, show the presence of spherical Pd nano particles with mean particle size in the range 5.0 to 6.0 nm (Table 1), with the exception of $Pd_{0.8}Au_{0.2}/TiO_2$ catalyst (3.9 nm), indicating the perceptible ensemble effect at this composition.

Pd-Au bimetallic catalysts are known[15,21,22] to form alloys, as indicated by DRS profiles, involving charge transfer between Pd and Au. Electronic interactions between Pd and Au are considered as a two way

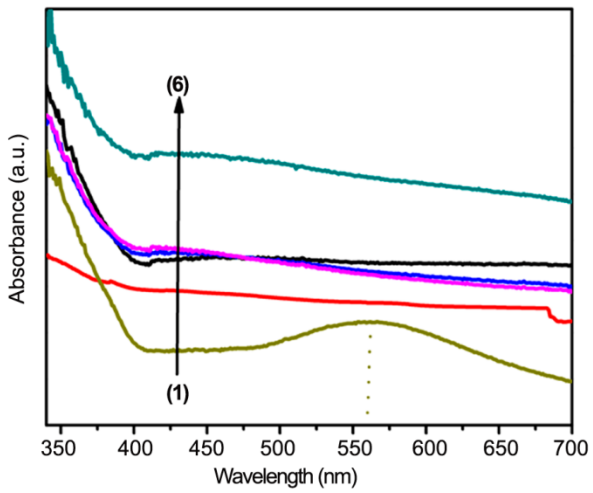

Fig. 1 — Diffuse reflectance spectra for $Pd_{(1-x)}Au_x$ series of catalysts: Au/TiO_2 (1), $Pd_{0.9}Au_{0.1}/TiO_2$ (2), Pd/TiO_2 (3), $Pd_{0.88}Au_{0.12}/TiO_2$ (4), $Pd_{0.8}Au_{0.2}/TiO_2$ (5), and, $Pd_{0.85}Au_{0.15}/TiO_2$ (6).

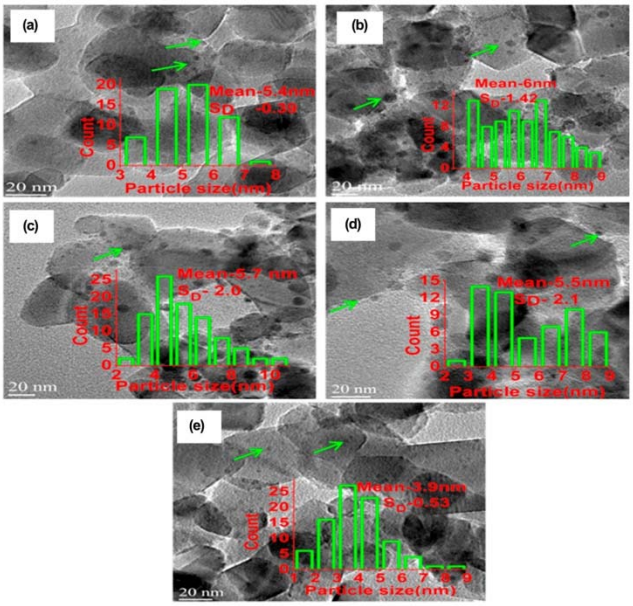

Fig. 2 — Transmission electron micrographs for $Pd_{(1-x)}Au_x$ series of catalysts (a) Pd/TiO_2, (b) $Pd_{0.9}Au_{0.1}/TiO_2$, (c) $Pd_{0.88}Au_{0.12}/TiO_2$, (d) $Pd_{0.85}Au_{0.15}/TiO_2$ and (e) $Pd_{0.8}Au_{0.2}/TiO_2$.

Table 1 — Characterization and activity data for $Pd_{(1-x)}Au_x$ series of catalysts

Catalysts	Particle size (nm)	T_{max} (°C)	Rate (10^{-6}mol/s)	TOF ($\times 10^{-3}$ s^{-1})
Pd	5.4	64.7	0.9	16.0
$Pd_{0.9}Au_{0.1}$	6.0	66.2	2.4	65.0
$Pd_{0.88}Au_{0.12}$	5.7	65.2	1.2	29.0
$Pd_{0.85}Au_{0.15}$	5.5	66.0	0.96	26.0
$Pd_{0.8}Au_{0.2}$	3.9	60.4	1.6	30.0

rates of hydrogenation calculated at 20±1% 1-heptyne conversion at 313 K

process, with Au gaining *sp* type electrons and losing *d* electrons while Pd loses *sp* electrons and gains *d* electrons[23,24]. This aspect is reflected in the XPS (Fig. 3) binding energy (BE) data for $Pd_{(1-x)}Au_x$ series of catalysts presented in Table 2.

Mono metallic Pd/TiO_2 displays XPS peak at 335.8 eV corresponding to Pd $3d_{5/2}$ energy level, which is close to the BE value (335.5 eV) reported for Pd/TiO_2-P-25[26]. With the addition of Au, the binding energy values for Pd $3d_{5/2}$ energy level tend to decrease, due to charge transfer from Au to Pd, thus altering its *d*-band character[23,24,26,27]. Correspondingly, BE values for Au $4f_{7/2}$ (Fig. S2) also decrease (with respect to BE value of 84.2 eV reported for Au/TiO_2) when Au content increases in the bi-metallic catalysts. Similar charge redistribution in Pd-Au alloys[23,24] and Pd-Au nano size catalysts supported on rutile titania nano rods[28] and in mixed anatase & rutile titania nano sheets[29], resulting in the lowering of XPS binding energy values for both Pd and Au, with respect to the respective mono metallic systems, have been observed earlier. Lower binding energy values for both Pd & Au in this case could be due to two way charge transfer prevalent in Pd-Au bimetallic system[23,24]. Such changes in *d*-band character of Pd could lead to weak chemisorptions of reactants/ products[24], vis-à-vis mono metallic Pd, thus influencing both activity and selectivity due to facile desorption of olefins.

TPR patterns for $Pd_{(1-x)}Au_x$ series of catalysts are presented in Fig. 4, wherein hydrogen evolution due to decomposition of the Pd hydride is observed for all catalysts of the series.

According to Bonarowska *et al.*[30] the characteristics of the Pd hydride decomposition peak (peak shape, distortion, peak maxima, and intensity) in Pd based bimetallic catalysts are governed by Pd crystallite size[31], alloy formation[32] and type of support and promoters[33]. As observed in Fig. 4, only one sharp peak with T_{max} ~65–70 °C (Table 1), without

Table 2 — XPS binding energy data for $Pd_{(1-x)}Au_x$ and Pd-M series of catalysts

Catalysts	Pd $3d_{5/2}$ (eV)	Au $4f_{7/2}$ (eV)	Ag $3d_{5/2}$ (eV)	Cu $2p_{3/2}$ (eV)
Pd	335.8	-	-	-
$Pd_{0.9}Au_{0.1}$	335.6	84	-	-
$Pd_{0.88}Au_{0.12}$	334.5	83.8	-	-
$Pd_{0.85}Au_{0.15}$	334.9	83.7	-	-
$Pd_{0.8}Au_{0.2}$	334.4	82.5	-	-
$Pd_{0.9}Ag_{0.1}$	334.5	-	366.6	-
$Pd_{0.9}Cu_{0.1}$	334.6	-		932.6

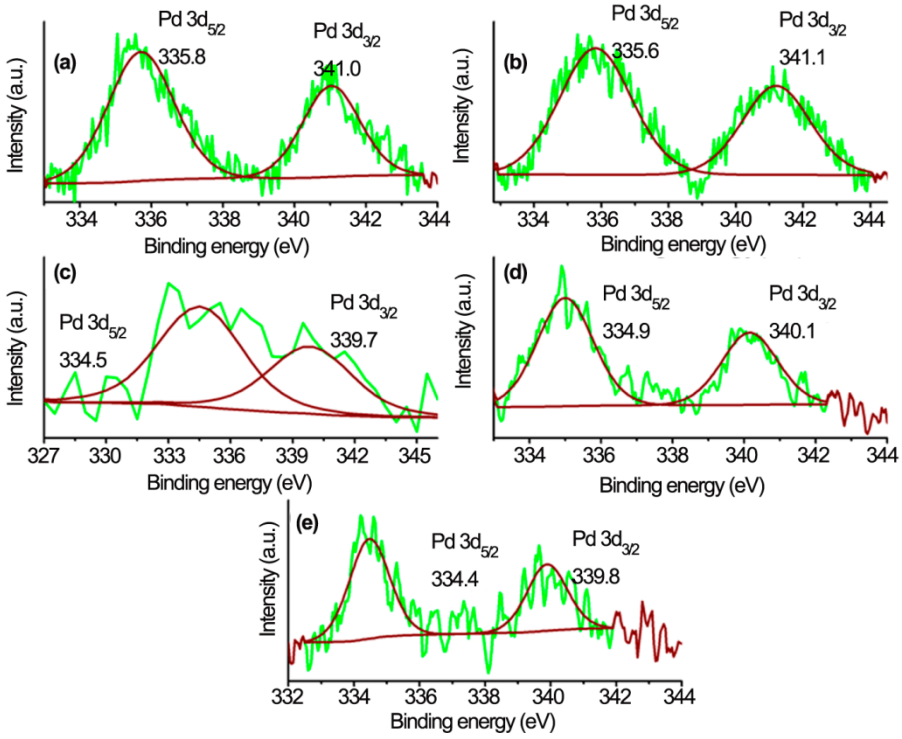

Fig. 3 — XPS profiles for Pd $3d_{5/2}$ level for $Pd_{(1-x)}Au_x$ series of catalysts: (a) Pd/TiO_2, (b) $Pd_{0.9}Au_{0.1}/TiO_2$, (c) $Pd_{0.88}Au_{0.12}/TiO_2$, (d) $Pd_{0.85}Au_{0.15}/TiO_2$ and (e) $Pd_{0.8}Au_{0.2}/TiO_2$.

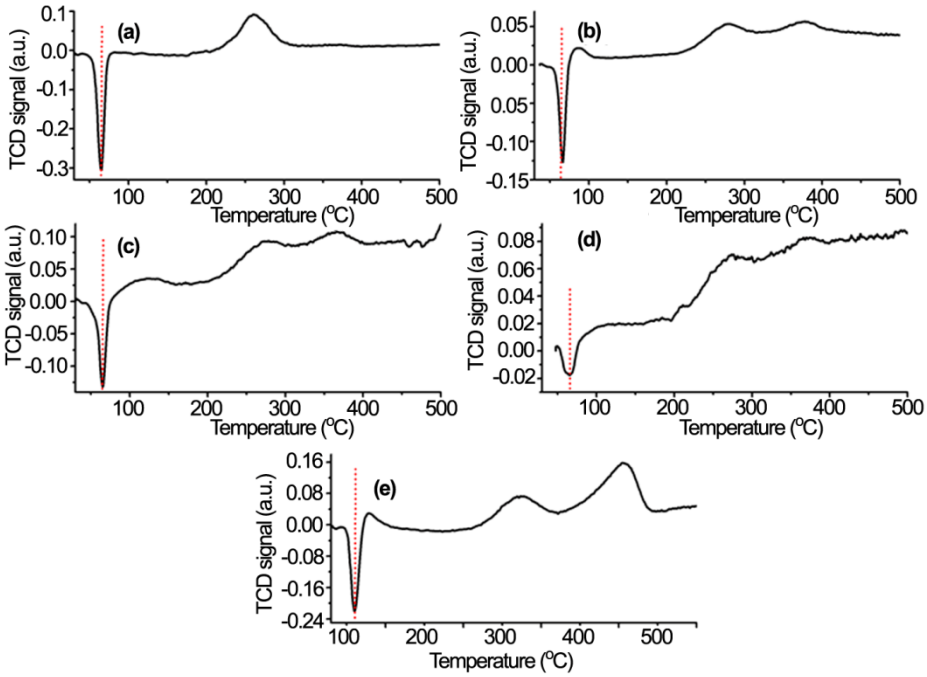

Fig. 4 — TPR patterns for $Pd_{(1-x)}Au_x$ series of catalyst: (a) Pd/TiO_2, (b) $Pd_{0.9}Au_{0.1}/TiO_2$, (c) $Pd_{0.88}Au_{0.12}/TiO_2$, (d) $Pd_{0.85}Au_{0.15}/TiO_2$ and (e) $Pd_{0.8}Au_{0.2}/TiO_2$.

any distortion, is observed in all catalysts of the series, indicating that Pd crystallites are mono dispersed and small in size, which is actually the case, according to TEM data. However, the intensity of the hydride decomposition peaks decrease as Au content increases, indicating that in presence of Au, Pd hydride formation is retarded. Since the Pd crystallites sizes in the series are nearly the same, the observed decrease in hydride peak intensity could be ascribed to the electronic interactions between Pd and Au leading to alloy formation.

Data on 1-heptyne conversion and selectivity for heptene, measured at 313 K at different time intervals for all $Pd_{(1-x)}Au_x$ series of catalysts, are presented in Figs S3 and S4 respectively. Addition of Au to Pd brings about significant increase in 1-heptyne conversion and is dependent on Pd-Au composition. Table 1 gives intrinsic activity data for $Pd_{(1-x)}Au_x$ series of catalysts, expressed in terms of TOF. Rates of 1-heptyne hydrogenation (measured at 313 K at 20±1% heptyne conversion) and Pd dispersion values calculated from TEM crystallite sizes were used for computing TOF values.

Addition of Au to Pd increases the intrinsic activity, as revealed by TOF values and maximum improvement in TOF with respect to mono metallic Pd/TiO_2, is observed with the composition, $Pd_{0.9}Au_{0.1}$. In the absence of any significant variation in Pd crystallite size, the observed improvement in intrinsic activity could be due to the charge transfer between Au and Pd, as evidenced by DRS and XPS data. Lowering of Pd $3d_{5/2}$ BE with addition of Au to Pd signifies, in general, a decrease in the interaction energy or weak adsorption of 1-heptyne vis-à-vis adsorption on mono metallic Pd. This leads to an increase in activity with $Pd_{0.9}Au_{0.1}$. However, further decrease in BE with increasing Au content lowers the activity, possibly due to two factors, weaker adsorption of 1-heptyne and ensemble effect on adsorption of hydrogen. At higher Au loading, ensemble effect could reduce contiguous Pd sites, thus limiting the availability of active surface hydrogen species required for hydrogenation. Takehiro *et al.*[34] have carried out theoretical as well as experimental studies on adsorption of hydrogen on bimetallic Pd-Au (111) surface alloys and have observed that 'critical ensemble' of 4 Pd atoms/Pd_4 tetramer is required for adsorption of hydrogen. Reduction in the uptake of hydrogen by nano sized Pd-Au bimetallic catalysts supported on CNT, with respect to the corresponding mono metallic Pd, has been reported by Wang *et al.*[35]. Thus, interplay of ligand as well as ensemble effects leads to an optimum $Pd_{(1-x)}Au_x$ composition. Nearly 100% selectivity for heptene formation is observed in all $Pd_{(1-x)}Au_x$ series of catalysts (Fig. S4), up to 60 min

indicating that selectivity is not altered with the addition of Au under the present experimental conditions.

Based on this study, another series of catalysts, with composition $Pd_{0.9}M_{0.1}$ where M = Cu, Ag and Au, were prepared and investigated to understand the role of group IB elements as promoters for this reaction.

$Pd_{0.9}M_{0.1}/TiO_2$ (M = Cu, Ag Au) series of bimetallic catalysts

X-Ray diffractograms for $Pd_{0.9}M_{0.1}$ (M = Cu, Ag Au) series catalysts do not display any significant change since the loading of the second metals is low. DRS profiles (Fig. 5) also do not display the characteristic SPR bands due to Ag & Au, while the corresponding mono metallic catalysts reveal distinct SPR bands at 429 nm and 562 nm respectively. Absence of SPR bands indicates alloy formation between Pd and Ag and Pd and Au[15,21,22].

TEM images for monometallic Pd and bimetallic Pd-M catalysts (Fig. 6) reveal the presence of spherical Pd nano particles with mean particle size in the range of 5–6 nm (Table 3).

Changes in the *d*-band character of Pd brought out by addition of group IB elements are reflected in the XPS (Fig. 7) studies on $Pd_{0.9}M_{0.1}$ (M = Cu, Ag Au) series of catalysts. Binding energy (BE) values along with other characteristics of the bi-metallic catalysts are given in Table 2. With respect to the BE value of 335.8 eV for Pd $3d_{5/2}$ core level for Pd/TiO_2, the corresponding values for Pd-Au, Pd-Ag and Pd-Cu are lower, at 335.6, 334.5 and 334.6 eV respectively, indicating charge transfer from promoter elements to Pd, which is in coherence with earlier reports[23-27,36]. Though BE for Pd $3d_{5/2}$ in Pd-Ag is less by 1 eV, with

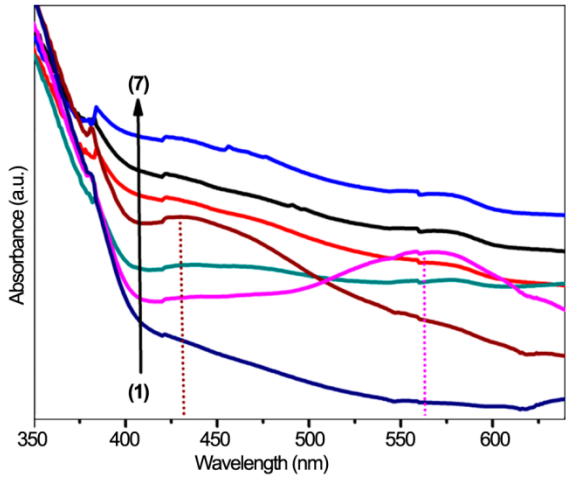

Fig. 5 — Diffuse reflectance spectra for Pd-M series of catalysts: Cu/TiO_2 (1), Au/TiO_2 (2), $Pd\text{-}Cu/TiO_2$ (3), Ag/TiO_2 (4), $Pd\text{-}Au/TiO_2$ (5), Pd/TiO_2 (6) and $Pd\text{-}Ag/TiO_2$ (7).

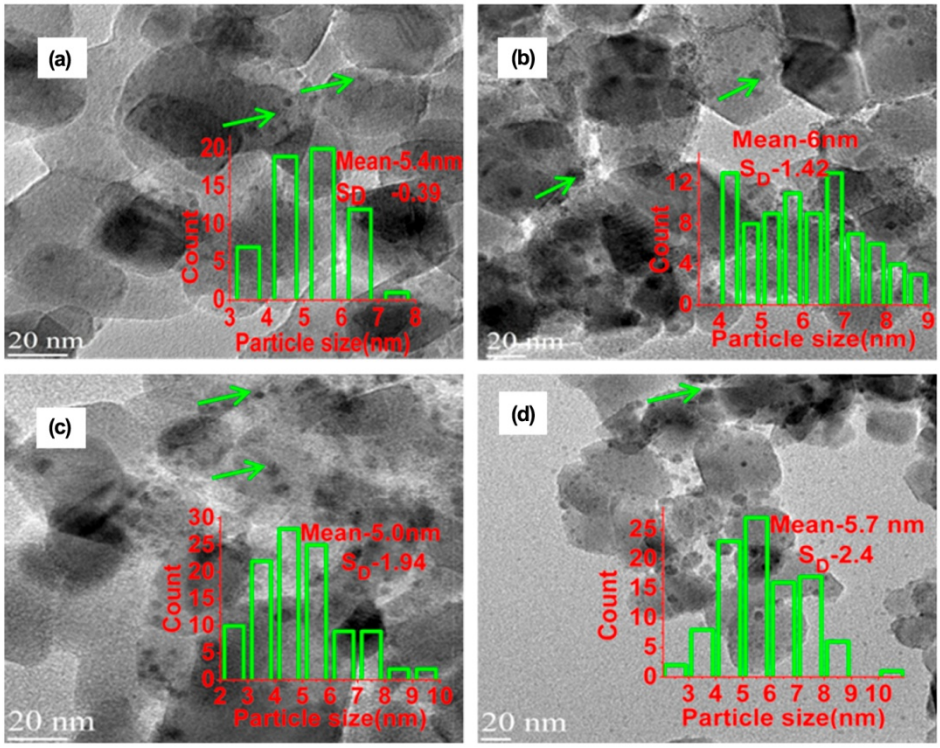

Fig. 6 — Transmission electron micrographs for Pd-M series of catalysts: (a) Pd/TiO_2, (b)$Pd\text{-}Au/TiO_2$, (c) $Pd\text{-}Ag/TiO_2$ and (d) $Pd\text{-}Cu/TiO_2$.

respect to that for mono metallic Pd, the activity for Pd-Ag is less than that for Pd-Au. This aspect needs further investigation. Shifts in BE values for group IB metals in the bimetallic catalysts (Table 2) vary, depending on the nature of the metal. BE value of 932.6 eV for Cu $2p_{3/2}$ in $Pd_{0.9}Cu_{0.1}$ is close to the value observed for Cu^0 in mono metallic Cu/TiO_2[37]. BE value of 366.6 eV observed for Ag $3d_{5/2}$ in Pd-Ag is close to that (366.3 eV) for Ag^{2+} supported on TiO_2-P-25[38], possibly due to exposure to atmospheric oxygen. As reported earlier, BE for Au $4f_{7/2}$ is lower (–0.2 eV) at 84.0 eV compared to 84.2 eV reported for Au/TiO_2. Accordingly the interaction energies for adsorption of 1-heptyne on these bimetallic catalysts are expected to vary.

TPR patterns for $Pd_{0.9}M_{0.1}$ (M = Cu, Ag Au) series of catalysts presented in Fig. 8 prominently display characteristic hydride decomposition peaks.

Table 3 — Characterization and activity data for Pd-M series of catalysts

Catalysts	Particle size (nm)	T_{max} (°C)	Rate (10^{-6} mol/s)	TOF ($\times10^{-3}$ s^{-1})
Pd	5.4	64.7	0.74	19
$Pd_{0.9}Au_{0.1}$	6.0	66.2	1.72	47
$Pd_{0.9}Ag_{0.1}$	5.0	69.7	0.87	20
$Pd_{0.9}Cu_{0.1}$	5.7	67.1	0.87	22

rates of hydrogenation calculated at 20±1% 1-heptyne conversion at 303 K

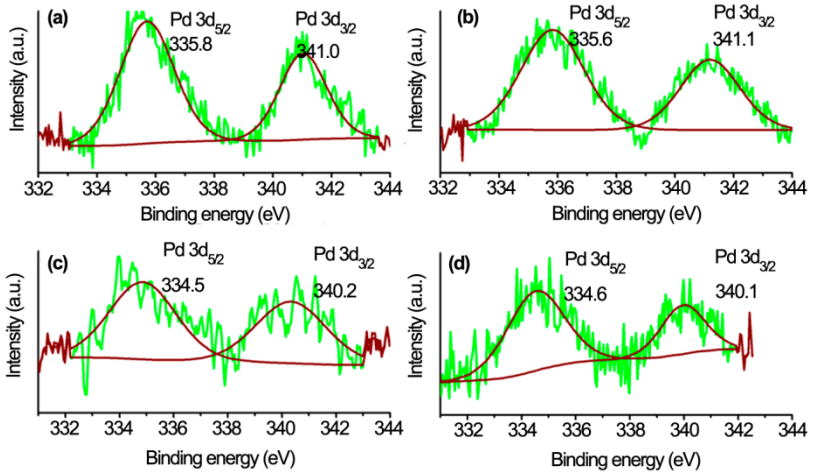

Fig. 7 —XPS profiles for Pd $3d_{5/2}$ level for Pd-M series of catalysts: (a)Pd/TiO_2, (b)$Pd-Au/TiO_2$, (c)$Pd-Ag/TiO_2$ and (d) $Pd-Cu/TiO_2$.

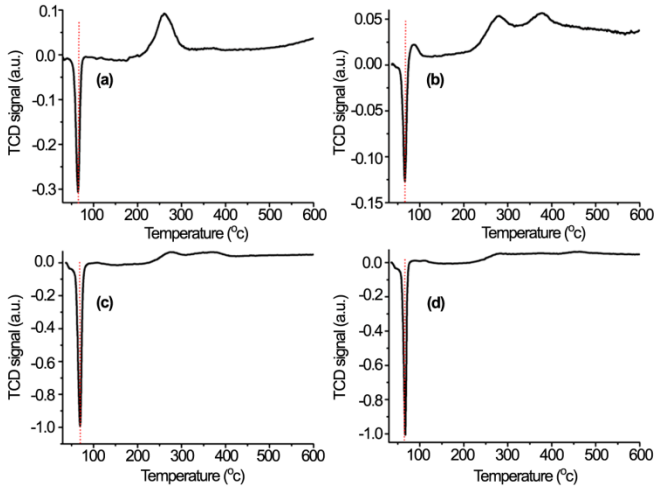

Fig. 8 — TPR patterns for Pd-M series of catalysts: (a) Pd/TiO_2, (b) $Pd-Au/TiO_2$, (c)$Pd-Ag/TiO_2$ and (d) $Pd-Cu/TiO_2$.

As observed with the $Pd_{(1-x)}Au_x$ series of catalysts, the peaks are sharp without any distortion, with T_{max} in the range 66–70 °C (Table 3), indicating the presence of mono dispersed small bi-metallic clusters. However, the intensity of peaks vary, depending on the second metal used, with Pd-Au displaying maximum reduction in the intensity of hydride decomposition peak, indicating the degree of alloying and its effect on hydride formation. Composition of the bimetallic catalyst may also affect the hydride formation. In the TPR for $Pd_{0.9}$-$Cu_{0.1}/Al_2O_3$ catalyst Cai *et al.*[39] observed hydride decomposition at 70 °C, but not with the catalysts having higher Cu content ($Pd_{0.8}Cu_{0.2}$ and $Pd_{0.5}Cu_{05}$).

Data on conversion of 1-heptyne and selectivity to heptene, at different time intervals and reaction temperatures, on $Pd_{0.9}M_{0.1}$ (M = Cu. Ag &Au) series of catalysts, are presented in Figs S5 and S6 respectively. Table 3 presents crystallite size, rates of hydrogenation at 303 K and the intrinsic activity, as revealed by TOF values, for the three bimetallic catalysts vis-à-vis mono metallic Pd/TiO_2. All TOF values were calculated based on the rates for hydrogenation at 20±1% conversion of 1-heptyne. Maximum TOF value is displayed by $Pd_{0.9}Au_{0.1}$ while $Pd_{0.9}Ag_{0.1}$ and $Pd_{0.9}Cu_{0.1}$ exhibit nearly the same activity. Nearly 100% selectivity for heptene formation is observed with all the Pd-M bimetallic catalysts under the present experimental conditions. However, during extended runs up to 120 min after the complete conversion of 1-heptyne, only a small drop in heptene selectivity is observed which is much less, in comparison with a relatively steep drop observed for mono metallic Pd. A typical run data for $Pd_{0.9}Cu_{0.1}/TiO_2$ versus Pd/TiO_2 is illustrated in Fig. S7. It is thus clear that bimetallic catalysts ensure higher heptene selectivity at high 1-heptyne conversion levels as well.

Higher activity and selectivity of Pd-Au catalysts (with varying compositions) has been observed for other reactions like oxidation of CO[40], hydro de-chlorination[41], syntheses of H_2O_2[42] and vinyl acetate[43]. Ensemble (geometric) as well as ligand (electronic) effects are considered to be responsible for the improvement in activity of Pd-Au catalysts depending upon the reaction with both being effective simultaneously[44].

Recently, Liu *et al.*[45] have reported high activity, selectivity and stability of Pd-Au single atom alloy (SAA) catalysts for liquid phase hydrogenation of 1-hexyne at 5 bar pressure, while in the present work, the reaction has been carried out at atmospheric pressure. A comparative study of mono and bimetallic catalysts (Pd-M, M = Cu, Ag, Au) for 1-heptyne hydrogenation is lacking so far, though such studies for selective hydrogenation of acetylene in ethylene rich streams have been reported. Zhang *et al*.[46] have observed that silica supported Pd-Au and Pd-Ag catalysts exhibit comparable activity and selectivity trends for selective hydrogenation of acetylene, wherein only ensemble effects were evident.

Introduction of atoms with different sizes, Ag (144pm), Au (144pm) and Cu (128pm), into Pd (138 pm) lattice and the consequent lattice strain could induce changes in the *d*-band character of Pd[47] and hence the nature of adsorption/reactivity of acetylene. Such changes at atomic/electronic levels could be studied in detail with the help of theoretical/DFT calculations. In the case of Ni-M catalysts (M = Cu, Ag, Au) DFT calculations have shown that bi-metallic Ni-Au, with lowest adsorption energy for acetylene, in comparison with Ni-Ag, Ni-Cu and mono metallic Ni catalysts, displays maximum activity for acetylene conversion. Similar DFT calculations have been carried out by the same authors[48] on Pd (211)-M (M = Cu, Ag and Au) catalysts. Based on the difference between the adsorption energy for ethylene and the energy barrier for ethylene hydrogenation, the authors have shown that Pd-Ag and Pd-Au display higher selectivity for ethylene formation vis-à-vis Pd-Cu. In a series of publications on selective hydrogenation of acetylene on Pd-M (M = Cu, Ag Au) single atom alloy (SAA) catalysts with M:Pd atomic ratio is in the range (1: 0.006 to 0.06), Pei *et al.*[49-51] have observed that Pd-Cu is more active than Pd-Ag and Pd-Au. It is proposed that high activity observed for Pd-Cu is due to the atomic size of Cu, which facilitates proper distance between isolated Pd atoms, while the sizes of Ag and Au may not do so[51]. This is in contrast to the conclusions arrived at by Yang *et al.*[47,48] on Ni and Pd based bimetallic catalysts.

Our experimental results on 1-heptyne hydrogenation are in accordance with those reported by Yang *et al.* on Ni-M catalysts[47,48] wherein Ni-Au catalyst displays maximum activity for hydrogenation of acetylene. Maximum activity (TOF) for hydrogenation of 1-heptyne in the present work is displayed by $Pd_{0.9}Au_{0.1}$. Results on DRS and XPS studies and the atomic size data on Pd, Cu, Ag and Au

indicate the influence of both ligand as well as ensemble effects in Pd-Au bimetallic catalyst in achieving higher activity and selectivity at higher conversions.

Conclusions

Selective hydrogenation of 1-heptyne to heptene has been investigated on two series of bimetallic catalysts, $Pd_{(1-x)}Au_x$ and Pd_mM_n, (M = Cu, Ag and Au) supported on TiO_2-P-25, at atmospheric pressure and temperature range 293–313 K. DRS and XPS studies reveal nano scale alloy formation between Pd and the promoter elements in both series of catalysts, resulting in redistribution of charges which retards the formation of Pd hydride. In $Pd_{(1-x)}Au_x$ series, maximum activity, expressed as TOF, is observed with the catalyst composition, $Pd_{0.9}Au_{0.1}$. In $Pd_{0.9}M_{0.1}$ (M = Cu, Ag Au) series, the activity pattern follows the trend: Pd-Au > Pd-Ag = Pd-Cu > Pd. Complete selectivity towards heptene is observed in both series of catalysts up to 60 min of reaction time. Pd-M bi-metallic catalysts ensure higher heptene selectivity at high 1-heptyne conversion levels beyond 60 min. Interplay of ligand as well as ensemble effects, acting simultaneously, influence the adsorption and activation of 1-heptyne, leading to the observed activity patterns, with Pd-Au displaying maximum activity and selectivity.

Supplementary Data

Supplementary data associated with this article are available in the electronic form at http://www.niscair.res.in/jinfo/ijca/IJCA_58A(02)271-280_SupplData.pdf.

Acknowledgement

The authors would like to thank the Department of Science and Technology, Govt of India, for establishing the research facilities at National Centre for Catalysis Research (NCCR) and IIT Madras, for providing infrastructure support for the Centre.

References

1 Ulan J G, Maier W F & Smith D A , *J Org Chem*, 52 (1987) 3132.
2 Crespo Quesada M, Cárdenas Lizana F, Dessimoz A L & Kiwi Minsker L, *ACS Catal*, 2 (2012) 1773.
3 (a) McCue A J & Anderson J A, *Front Chem Sci Eng*, 9 (2015) 142, (b) Nikolaev S A, Leonid N Z, Smirnov V V, Vyacheslav A A & Zanaveskin K L , *Russ Chem Rev*, 78 (2009) 231.
4 Yarulin A, Yuranov I, Cárdenas-Lizana F, Alexander D T L & Kiwi-Minsker L, *Appl Catal A: Gen*, 478 (2014)186.
5 (a) Montsch T, Heuchel M, Traa Y, Klemm E & Stubenrauch C, *Appl Catal A:Gen*, 539 (2017) 19, (b) Nijhuis T A, van Koten G & Moulijn J A, *Appl Catal A: Gen*, 238 (2003) 259, (c) Yarulin A, *Catalyst development for hydrohenation of functionalized alkynes and nitroarenes*, Ph D Thesis, Ecole Polytechnique Fédérale de Lausanne, Switzerland, 2014.
6 Insorn P, Suriyaphaparkorn K & Kitiyanan B, *Chem Engg Trans*, 32 (2013) 847.
7 (a) Lederhos C R, Badano J M, Quiroga M E, L'Argentière P C & Coloma-Pascual F, *Quím Nova*, 33 (2010) 816, (b) Lederhos C R, Maccarrone M J, Badano J M, Torres G, Coloma Pascual F & Yori J C, *Appl Catal A Gen*, 396 (2011) 170.
8 Karakhanov E A, Maximov A L, Zolotukhina A V, Yatmanova N & Rosenberg E, *Appl Organo Met Chem*, 29 (2015) 777.
9 Lederhos C R, Badano J M, Carrara N, Coloma Pascual F, Almansa M C & Liprandi D, *Sci World J*, 528453 (2013) 1.
10 Lederhos C R, L'Argentière P C & Fígoli N S, *Indl & Eng Chem Res*, 44 (2005) 1752.
11 Putdee S, Mekasuwandumrong O, Soottitantawat A & Panpranot J, *J Nano Sci Nano technol*, 13 (2013) 3062.
12 Lederhos C R, L'Argentière P C, Coloma Pascual F & Fígoli N S, *Catal Lett* , 110 (2006) 23.
13 (a) Kittisakmontree P, Yoshida H, Fujita S I, Arai M & Panpranot, *J Catal Comm*, 58 (2015) 70, (b) Sirikajorn T, Mekasuwandumrong O, Praserthdam P, Goodwin J G & Panpranot J, *Catal Lett*, 126 (2008) 313.
14 Carrara N, Badano J M, Betti C, Lederhos C, Rintoul I & Coloma-Pascual F, *Catal Comm*, 61 (2015) 72.
15 Kittisakmontree P, Pongthawornsakun B, Yoshida H, Fujita S I, Arai M & Panpranot J, *J Catal*, 297 (2013) 155.
16 Klasovsky F, Claus P & Wolf D, *Top Catal*, 52 (2009) 412.
17 (a) Pongthawornsakun B, Fujita S i, Arai M, Mekasuwandumrong O & Panpranot J , *Appl Catal A Gen*, 467 (2013) 132, (b) Mekasuwandumrong O, Somboonthanakij S, Praserthdam P & Panpranot J, *Ind Eng Chem Res*, 48 (2009) 2819.
18 Chen L J, Wan C C & Wang Y Y, *J Coll Interf Sci*, 297 (2006)143.
19 Isaifan R J, Dole H A E, Obeid E, Lizarraga L, Vernoux P & Baranova E A, *Electrochem Solid State Lett*, 5 (2012) E14.
20 Dash P, Dehm N A & Scott R W J, *J Mol Catal A Chem*, 286 (2008) 114.
21 Scott R W J, Wilson O M, Oh S K, Kenik E A & Crooks R M, *J Am Chem Soc*, 126 (2004) 15583.
22 Lee Y S, Jeon Y & Oh S J, *J Kor Phys Soc*, 37 (2000) 451.
23 (a) Gao F & Goodman D W, *Chem Soc Rev*, 24 (2012) 8009, (b) Yi C W, Luo K, Wei T & Goodman D W, *J Phys Chem B*, 109 (2005) 18535.
24 Shen W J, Okumura M, Matsumura Y & Haruta M, *Appl Catal A Gen*, 213 (2001) 225.
25 Chen D, Li C, Liu H, Ye F & Yang J, *Nat Sci Rep*, 5 (2015) 11949.
26 Nutt M O, Heck K N, Alvarez P & Wong M S, *Appl Catal B*, 69 (2006) 115.
27 Konuspayeva Z, Afanasiev P, Nguyen T S, Di Felice L, Morfin F & Nguyen N T, *Phys Chem Chem Phys*, 17 (2015) 28112.
28 Xin Y, Wu L, Ge L, Han C, Li Y & Fang S, *J Mater Chem A*, 3 (2015) 8659.
29 Bonarowska M, Pielaszek J, Juszczyk W & Karpiński Z, *J Catal*, 195 (2000) 304.

30 Boudart M & Hwang H S, *J Catal*, 39 (1975) 44.
31 Joice B J, Rooney J J, Wells P B & Wilson G R, *Faraday Soc* ,41 (1966) 223.
32 (a) Chang T C, Chen J J & Yeh C T , *J Catal*, 96 (1985) 51, (b) Benedetti A, Fagherazzi G, Pinna F, Rampazzo G, Selva M & Strukul G, *Catal Lett*, 10 (1991) 215.
33 Takehiro N, Liu P, Bergbreiter A, Norskov J K & Behm R J , *Phys Chem Chem Phys*, 16 (2014) 23930.
34 Wang S, Xin Z, Huang X, Yu W, Niu S & Shao L, *Phys Chem Chem Phys*, 19 (2017) 6164.
35 Fu G T, Liu C, Zhang Q, Chen Y & Tang Y W, *Nat Sci Rep*, 5 (2015) 13703.
36 Li F, Cao B, Ma R, Liang J, Song H & Song H , *Can J Chem Eng*, 94 (2016) 1368.
37 Kowalska E, Yoshiiri K, Wei Z, Zheng S, Kastl E & Remita H, *Appl Catal B*,178 (2015) 133.
38 Cai F, Yang L, Shan S, Mott D, Chen B & Luo J ,*Catalysts*, 6 (2016) 96.
39 (a) Gao F, Wang Y& Goodman D W, *J Am Chem Soc*, 131 (2009) 5734 , (b) Gao F, Wang Y & Goodman D W, *J Phys Chem C*, 113 (2009) 14993, (c) Xu J, White T, Li P, He C, Yu J &Yuan W , J Am *Chem Soc*, 132 (2010) 10398.
40 Nutt M O, Heck K N, Alvarez P & Wong M S, *Appl Catal B*, 69 (2006) 115.
41 Edwards J K, Solsona B E, Landon P, Carley A F, Herzing A & Kiely C J, *J Catal*, 236 (2005) 69.
42 Yuan D, Gong X &Wu R , *J PhysChem C*, 112 (2008) 1539.
43 Liu P &Norskov J K , *Phys Chem Chem Phys*, 3 (2001) 3814.
44 Liu J, Shan J, Lucci F R, Cao S ,Sykes E C H & Flytzani S M, *Catal Sci Tech*, 7 (2017) 4276.
45 Zhang Y, Diao W, Williams C T &Monnier J R, *Appl Catal A Gen*, 469 (2014) 419.
46 Mavrikakis M, Hammer B &Nørskov J K , *Phys Rev Lett*, 81 (1998) 2819.
47 Yang B, Burch R, Hardacre C, Headdock G & Hu P, *ACS Catal*, 2 (2012) 1027.
48 Yang B, Burch R, Hardacre C, Headdock G & Hu P, *J Catal*, 305 (2013) 264.
49 Pei G X, Liu X Y, Wang A, Li L, Huang Y & Zhang T, *New J Chem*, 38 (2014) 2043.
50 Pei G X, Liu X Y, Wang A, Lee A F, Isaacs M A & Li L, *ACS Catal*, 5 (2015) 3717.
51 Pei G X, Liu X Y, Yang X, Zhang L, Wang A & Li L, *ACS Catal*, **7** (2017) 1491.